remote sensing

MDPI

Article

MOD2SEA: A Coupled Atmosphere-Hydro-Optical Model for the Retrieval of Chlorophyll-a from Remote Sensing Observations in Complex Turbid Waters

Behnaz Arabi [1,*], Mhd. Suhyb Salama [1], Marcel Robert Wernand [2] and Wouter Verhoef [1]

[1] Faculty of Geo-Information Science and Earth Observation (ITC), Department of Water Resources, University of Twente, P.O. Box 217, 7500AE Enschede, The Netherlands; s.salama@utwente.nl (M.S.S.); w.verhoef@utwente.nl (W.V.)

[2] Department of Coastal Systems, Marine Optics and Remote Sensing, Royal Netherlands Institute for Sea Research (NIOZ), P.O. Box 59, 1790AB Den Burg, Texel, The Netherlands; marcel.wernand@nioz.nl

* Correspondence: b.arabi@utwente.nl or arabi.behnaz@gmail.com; Tel.: +31-534-874-288

Academic Editors: Magaly Koch and Prasad S. Thenkabail
Received: 20 June 2016; Accepted: 27 August 2016; Published: 1 September 2016

Abstract: An accurate estimation of the chlorophyll-a (Chla) concentration is crucial for water quality monitoring and is highly desired by various government agencies and environmental groups. However, using satellite observations for Chla estimation remains problematic over coastal waters due to their optical complexity and the critical atmospheric correction. In this study, we coupled an atmospheric and a water optical model for the simultaneous atmospheric correction and retrieval of Chla in the complex waters of the Wadden Sea. This coupled model called MOD2SEA combines simulations from the MODerate resolution atmospheric TRANsmission model (MODTRAN) and the two-stream radiative transfer hydro-optical model 2SeaColor. The accuracy of the coupled MOD2SEA model was validated using a matchup data set of MERIS (MEdium Resolution Imaging SpectRometer) observations and four years of concurrent ground truth measurements (2007–2010) at the NIOZ jetty location in the Dutch part of the Wadden Sea. The results showed that MERIS-derived Chla from MOD2SEA explained the variations of measured Chla with a determination coefficient of $R^2 = 0.88$ and a RMSE of 3.32 mg·m^{-3}, which means a significant improvement in comparison with the standard MERIS Case 2 regional (C2R) processor. The proposed coupled model might be used to generate a time series of reliable Chla maps, which is of profound importance for the assessment of causes and consequences of long-term phenological changes of Chla in the turbid Wadden Sea area.

Keywords: Chlorophyll-a; remote sensing; MERIS; atmospheric correction; MODTRAN; 2Seacolor; C2R; Wadden Sea

1. Introduction

Effective management of water quality in coastal regions and turbid waters requires accurate information about water quality parameter changes on prolonged time scales. Although this may sound simple, it is an extremely challenging task. One of the most important water quality parameters is chlorophyll-a (Chla) concentration, which is an important factor controlling light attenuation in the water column and is used as a measure of the eutrophic state [1]. Chla concentration is a very crucial factor to understanding the planetary carbon cycle [2] and is considered as an important indicator of eutrophication in marine ecosystems that may influence human life [3,4]. Chla abundance can be affected by anthropogenic nutrient supply from industrial and agricultural sources, where simultaneously the aquaculture industries and fisheries are influenced by Chla abundance [5].

Long-term monitoring of Chla concentration using field measurements and laboratory analysis requires conventional cruise surveys with satisfactory temporal and spatial coverage. Unfortunately, this is often not feasible for most coastal regions due to lack of financial resources and technical equipment while it is impossible in practice to collect in situ measurements for the whole regions using cruise measurements. The spatiotemporal coverage provided by remote sensing can considerably overcome some of these deficits in the current in situ monitoring programs for water quality parameters [6]. Satellite ocean color is especially important since it is the only remotely sensed property that directly identifies a biological component of the ecosystem [2]. Regarding the spatial and temporal sampling capabilities of satellite data, remote sensing of ocean color is considered as the principal source of data for investigating long-term changes in Chla concentration and phytoplankton biomass in many coastal areas' estuaries [7].

The maintenance of a good environmental status in European coastal regions and sea has become a crucial concern embodied in European regulations (Marine Strategy Framework Directive, Directive 2008/56/EC of the European Parliament and of the Council, "establishing a framework for community action in the field of marine environmental policy") [8]. One of the most important European coastal zones which has aroused increasing attention from all of Europe is the Wadden Sea. For the assessment of the current role of the Wadden Sea as a source of Chla and organic matter, and for the ongoing discussion on eutrophication problem areas, it is of great interest to obtain more detailed knowledge on the phytoplankton and Chla changes and their regulating factors in this turbid coastal region of the North Sea [9]. In addition, monitoring of this area is mandatory due to its nature reserve status and its July 2009 inclusion on the UNESCO World Heritage List [10]. Recently some research into the analysis of long-term variations and trends in the optically active substances (Chla, Suspended Particulate Matter (SPM), Colored Dissolved Organic Matters (CDOM)) and water color changes using in situ measurements have been conducted over different parts of the Wadden Sea [11–14]. However, using satellite observations for Chla estimation remains problematic in this area due to its optical complexity and the critical application of an accurate atmospheric correction. Recent efforts show that researchers are confronted with two main problems in improving the accuracy of derived water parameter concentration using remote sensing techniques in the Wadden Sea. First, most atmospheric correction methods fail in this region [15,16]. Second, the general water property retrieval models do not work well in this complex turbid water [17,18]. Thus, the main purpose of this research is to tackle these two problems aiming to increase the accuracy of Chla concentration retrieval from earth observation data in this area.

1.1. Atmospheric Correction

Quality of the atmospheric correction is one of the most limiting factors for the accurate retrieval of water constituents from earth observation data in coastal waters [19]. The standard atmospheric correction method by Gordon and Wang [20] assumes a zero water-leaving reflectance due to high absorption by seawater in the near-infra-red (NIR) and can be performed by extrapolating the aerosol optical properties to the visible from the NIR spectral region [21]. This is not always the case when in turbid waters (which often are optically complex) [22], higher concentrations of Chla and SPM can cause a significant water-leaving reflectance in the NIR [23]. Indeed, most of the atmospheric correction methods fail in these areas due to the complexity of the recorded top of atmosphere (TOA) radiance signal at satellite images [24] as these signals are associated with aerosols from continental sources [25]. In addition, in coastal waters, photons from nearby land areas can enter the field-of-view of the sensor (the adjacency effect) and contribute to total NIR backscatter [26], whereas in shallow waters, TOA radiances can also be influenced by the bottom effect [10]. Consequently, the black pixel assumption tends to overestimate the aerosol scattered radiance and thus underestimates the water-leaving radiance in these areas [27]. In recent years, some studies have been conducted to improve the atmospheric correction over turbid waters [28–30]. For example, some efforts were made to improve the atmospheric correction method by assuming a zero water-leaving reflectance

in the shortwave infrared, even in the case of highly turbid waters [31,32]. However, in further studies, researchers found that for extremely high turbidities, even in the shortwave infrared region, the water-leaving reflectance was not absolutely equal to zero [33]. In addition, other studies focused on the non-negligible water-leaving reflectance assumption in the NIR [34,35]. For example, Carder et al. [36] investigated the ratio of water-leaving reflectance at two NIR bands. This ratio was either assumed constant [37] or estimated from neighboring pixels of open oceans [38]. Although the assumption of a known relationship between the values of water-leaving reflectance in two NIR bands is necessary, it is not sufficient. Indeed, accurate information about visibility and aerosol type is still needed [34]. Shen et al. [39] used the radiative transfer model MODTRAN to perform atmospheric correction for MERIS images over highly turbid waters. As shown by Verhoef and Bach [40], for an assumed visibility and aerosol type, MODTRAN can be used to extract the necessary atmospheric parameters to remove the scattering and absorption effects of the atmosphere and to obtain calibrated surface reflectance, as well as correcting the adjacency effects. However, this technique assumes a spatially homogeneous atmosphere [41], while in reality not only visibility but also the aerosol type may vary spatially within the extent of satellite images (in the presence of local haze variations). For example, in the case of coastal waters, some aerosol types (e.g., urban or rural) might exist in the regions close to the land and other pixels might have the maritime aerosol type. Consequently, the assumption of a homogeneous atmosphere may lead to wrong establishment of visibility and aerosol model in different parts of the image and may result in overestimation or underestimation of water constituent concentrations from ocean-color observations. The Case-2 regional (C2R) processor provided by ESA for MERIS L1 products in the MERIS regional coastal and case 2 water projects [42], performs atmospheric correction pixel by pixel and contains procedures for determining inherent optical properties that are delivered as MERIS L2 products, including reflectance, inherent optical properties (IOPs), and water quality parameters. However, the C2R processor may be invalid for very chlorophyll-rich waters like some eutrophic lakes [43] and for highly turbid waters [39]. In this paper, by applying radiative transfer modeling for the non-homogeneous atmosphere and comparing the results with the C2R processor, we tried to improve the atmospheric correction technique over this coastal area.

1.2. Hydro-Optical Model

After improving the atmospheric correction technique, water constituent concentration-dependent optical modeling of turbid waters is the next step. Improving the accuracy of water properties retrievals in coastal waters requires generic models that can be applied to these complex water bodies [44]. For open oceans, estimation of Chla from earth observation data is well established [45]. An empirical algorithm is in use that, with slight modifications for the actual band settings, has proven to work well for instruments like SeaWiFS (Sea-Viewing Wide Field-of-View Sensor), MODIS (Moderate Resolution Imaging Spectroradiometer) and MERIS [46–48]. However, satellite estimation of Chla concentration is still difficult for coastal waters, where Chla, SPM and CDOM occur in various mixtures which complicate the derivation of their concentrations from reflectance observations [49].

Therefore, there is a pressing need to develop, implement and validate a self-consistent, generic and operational retrieval model of water quality in turbid waters [49]. In this study, the forward analytical model known as 2SeaColor developed by Salama and Verhoef [50] was applied for the first time to retrieve Chla concentration in the Wadden Sea. The 2SeaColor model is based on the solution of the two-stream radiative transfer equations for incident sunlight and also performs well for turbid waters, while the commonly applied water quality algorithms might suffer from saturation in the presence of a high turbidity [44].

After defining the main problems of remote sensing of coastal waters described above, and motivated by the need for a high-quality, satellite-based long-term Chla retrieval in the turbid waters of the Wadden Sea, this research focused on the following objectives: (1) improving the accuracy of Chla concentration ($mg \cdot m^{-3}$) retrieval from MERIS data by applying a coupled MODTRAN−2SeaColor

model (MOD2SEA) for the Wadden Sea and (2) comparing the accuracy of the coupled MOD2SEA in performing atmospheric correction and retrieving Chla concentration values with the ESA standard C2R processor. The paper is arranged as follows. The case study is described first. Then, the datasets used for C2R and MODTRAN simulations as well as the 2SeaColor model are briefly introduced. Next, we validate the derived Chla concentration and water-leaving reflectance values for both MOD2SEA and C2R processor against the ground truth measurements at the NIOZ jetty station. Then, we evaluate the remote sensing (MOD2SEA and C2R) retrievals and compare the variation of MOD2SEA results with similar in situ studies in the Wadden Sea. Finally, we suggest some recommendations for further remote sensing studies in complex turbid waters like the Wadden Sea and discuss the applicability of this approach to other estuaries and satellite ocean color missions.

2. Materials and Methods

2.1. Study Area

The Dutch Wadden Sea is a coastal area located between the mainland of the Netherlands and the North Sea. The area is located between the Marsdiep near Den Helder in the southwest and the Dollard near Groningen in the northeast and comprises a surface area of 2500 km^2 (Figure 1). This region is a shallow, well-mixed tidal area that consists of several separated tidal basins. Each basin comprises tidal flats, subtidal areas and channels. Basins are connected to the adjacent North Sea by relatively narrow and deep tidal inlets between the barrier islands [51].

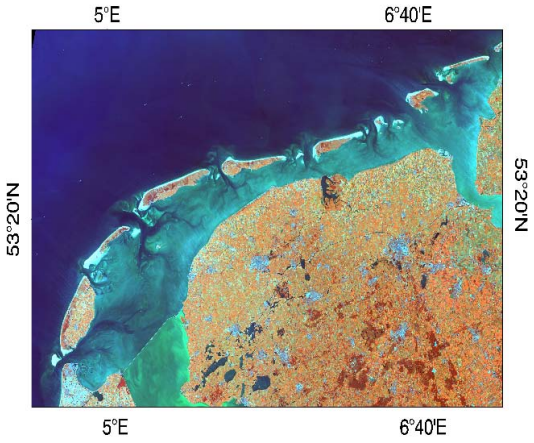

Figure 1. One Landsat-8 OLI image covering the Dutch Wadden Sea and parts of IJsselmeer lake acquired on 20 July 2016 (Color composite of red = band 5, green = band 3 and blue = band 1).

The high near-surface concentrations of water constituents as well as the spatial, tidal and seasonal variations of the optically active substances (Chla, SPM and CDOM) make this region an optically very complex area and a good representative for remote sensing studies in turbid coastal waters [10].

2.2. Ground Truth Dataset

The ground truth data have been extensively used to investigate the accuracy of remote sensing radiometric products (i.e., the remote sensing reflectance) from the recorded TOA radiance in satellite observations like MERIS images [52]. In this study, the ground truth above-water radiometric dataset was provided by the research jetty of the Royal Netherlands Institute for Sea Research (NIOZ) at Texel, located in the Dutch part of the Wadden Sea. Every quarter of an hour, radiometric color measurements of the water, sun and sky (including meteorological conditions), as well as Chla and mineral concentration, were recorded for over a decade [53]. The data were collected at the NIOZ jetty station (53°00′06″N; 4°47′21″E) [54], where the newest generation of hyperspectral radiometers was installed for "autonomous" monitoring of the Wadden Sea from 2001 until the present [53] (Figure 2).

The footprint size of the radiometer is less than a meter, and the viewing direction is not nadir but oblique, so the measurements on the ground are only partially representative of the nadir water reflectance from 300 m pixels as sensed by MERIS.

Figure 2. (**a**) The location at the NIOZ jetty sampling station in the western part of the Dutch Wadden Sea [54]; (**b**) The optical system mounted on a pole on the platform of the NIOZ jetty in the Wadden Sea [53].

In addition, specific inherent optical properties (SIOPs) of water constituents in the Wadden Sea were obtained from Hommersom et al. [11], who documented SIOP measurements in 2007 at 37 stations in this area.

2.3. Satellite Observations

The MERIS sensor, operational on board the European environmental satellite ENVISAT between 2002–2012, was primarily intended for ocean, coastal and continental water remote sensing. MERIS was an orbital sensor with 15 bands covering the spectral range from 400 to 950 nm and was succeeded by the Ocean and Land Color Instrument (OLCI) on board Sentinel-3 beyond 2015 [55]. The high sensitivity and large dynamic range of the MERIS sensor has been widely used for ocean and coastal water remote sensing [56–59]. In this study, ocean color data were obtained from ESA archive of MERIS images (full resolution: 300 m) covering the Wadden Sea during 2002–2012 (data provided by European Space Agency). MERIS has a revisit time of three days over the Dutch Wadden Sea at around 10:30 a.m. local time. The MERIS 1b image provides TOA radiance information and some environmental parameters for each pixel. Some of these environmental parameters (such as sun zenith angle (SZA), view zenith angle (VZA), relative azimuth angle (RAA), water vapor (H_2O) and ozone (O_3)) were used as input parameters to perform MODTRAN simulations in this study.

2.4. Ground Truth and Satellite Observation Data Matchups

Validation of ocean color products (i.e., biogeochemical parameters, inherent optical properties (IOPs) and water-leaving radiance), theoretically, should be performed from ground truth measurements acquired simultaneously to the satellite overpass over the same location (the so-called matchup points) [60]. In this study, the following criteria were used to find matchup points between satellite observations and ground truth measurements: (1) all available MERIS images over the Dutch part of Wadden Sea between 2002 and 2012 were checked to select the cloud-free images; (2) a narrow time window of $\pm$1 h was used; (3) five-by-five pixel kernels centered on the ground truth measurement coordinates were then extracted from the MERIS images using BEAM software (version 5.0) (no aggregation method was used to avoid possible spectral contamination); (4) finally, 35 suitable MERIS images were concurrent with ground truth-measured concentrations of Chla at the NIOZ jetty station during 2007–2010.

3. Methodology

The accuracy of the coupled MOD2SEA model in doing atmospheric correction and deriving Chla concentration values was evaluated against ground truth measurements and was compared with C2R results.

3.1. The Coupled MOD2SEA Model

The developed MOD2SEA method combined two lookup tables (LUTs) from 2SeaColor and MODTRAN as schematically shown in Figure 3.

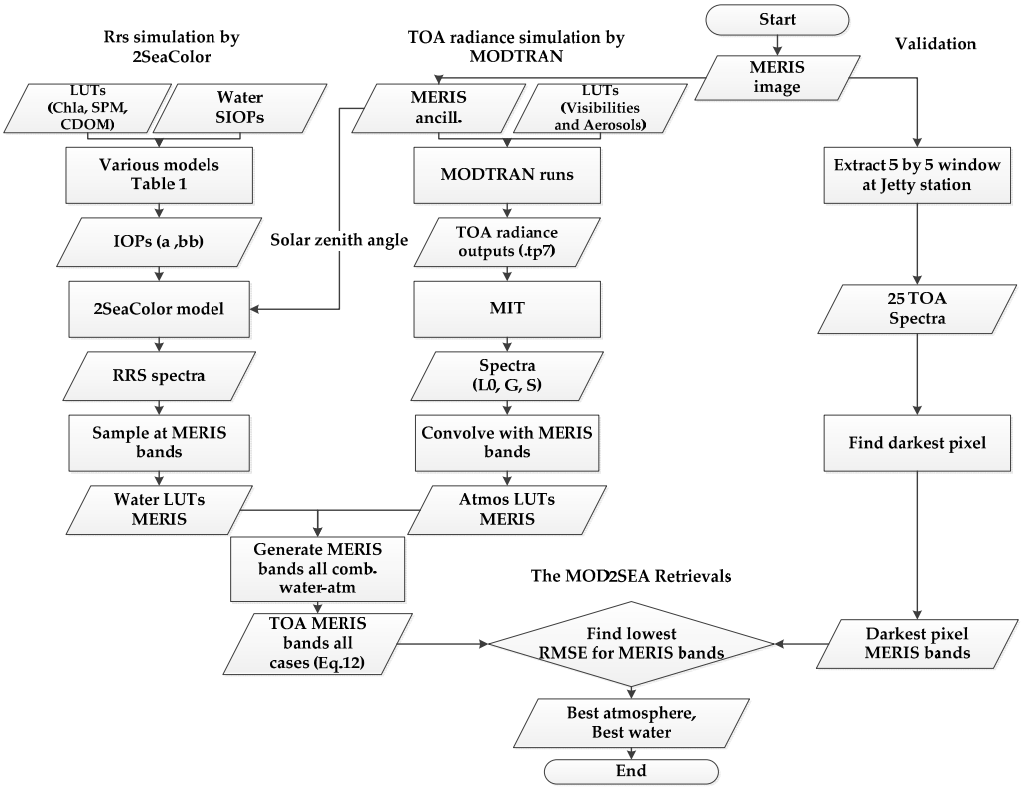

Figure 3. Diagram of the coupled MOD2SEA model (pixel based).

These LUTs were generated by simulating the water-leaving reflectance for varying ranges of the governing biophysical variables (with respect to range of these water quality variables at the NIOZ jetty station (Table 1)) and MODTRAN parameters based on different combinations of visibilities and aerosol models at specific viewing-illumination geometries for every MERIS image separately. Table 1 presents the LUT composition of the 2SeaColor model and the MODTRAN input variables in this assessment.

Table 1. Lookup table composition of MOD2SEA model.

LUT Variables	Range	Increment	Unit
Chla	0–150	5; 0.1	$mg \cdot m^{-3}$
SPM	0–150	5; 0.1	$g \cdot m^{-3}$
CDOM absorption at 440 nm	0–2.5	1; 0.1	m^{-1}
Visibility	5–50	1	km
Aerosol type	Rural, Maritime, Urban	-	-

The details on simulation of R_{RS} by the 2SeaColor model and TOA radiance by the MODTRAN radiative transfer code are described as follows:

3.1.1. Reflectance (R_{RS}) Simulation by 2SeaColor Forward Model

The 2SeaColor model is based on the solution of the two-stream radiative transfer equations including direct sunlight, as described by Duntley (1942, 1963) [61,62]. Both the analytical forward model and the inversion scheme are provided in detail in Salama and Verhoef [50]. The reflectance result predicted by the 2SeaColor model is r_{sd}^{∞}, the directional-hemispherical reflectance of the semi-infinite medium, which is linked to IOPs by Salama and Verhoef [50]:

$$r_{sd}^{\infty} = \frac{\sqrt{1+2x}-1}{\sqrt{1+2x}+2\mu_w} \tag{1}$$

where x is the ratio of backscattering to absorption coefficients ($x = b_b/a$), and μ_w is the cosine of the solar zenith angle beneath the water surface. The reflectance factor r_{sd}^{∞} can be approximated by $Q \times R(0^-)$ under sunny conditions, where $Q = 3.25$ and $R(0^-)$ is the irradiance reflectance beneath the surface [63], which can be converted to above-surface remote sensing reflectance (R_{RS}) by Lee et al. [64].

$$R_{RS} = \frac{0.52 \times R\left(0^-\right)}{1 - 1.7 \times R\left(0^-\right)} \tag{2}$$

Total absorption and backscattering coefficient of water constituents (a and b_b) were calculated using Equations (3) and (4) respectively [27,48].

$$a\left(\lambda\right) = a_w\left(\lambda\right) + a_{chl}\left(\lambda\right) + a_{nap}\left(\lambda\right) + a_{cdom}\left(\lambda\right) \tag{3}$$

$$b_b\left(\lambda\right) = b_{bw}\left(\lambda\right) + b_{b,chl}\left(\lambda\right) + b_{b,nap}\left(\lambda\right) \tag{4}$$

where the subscripts w, chl, nap and $cdom$ stand for water molecules, chlorophyll, non-algae particles and colored dissolved organic matter, respectively. As implemented in Salama and Shen [65], the absorption coefficients of the water constituents (a) are parameterized by (Bricaud et al. [66]; Lee et al. [67]; Lee et al. [68]). Also, the backscattering coefficients of the water constituents (b_b) were parametrized by (Doxaran et al. [69] and Morel et al. [70]).

Table 2. Summary of the used parameterizations.

Variable	Parametrization	Equation	Reference
Chla absorption	$a_{chl}\left(\lambda\right) = \left[a_0\left(\lambda\right) + a_1\left(\lambda\right) \times \ln a_{chl}\left(443\right)\right] \times a_{chl}\left(443\right)$ $a_{chl}\left(443\right) = 0.06 \times \left[Chl\right]^{0.65}$	(5)	[68]
CDOM absorption	$a_{cdom}\left(\lambda\right) = a_{cdom}\left(440\right) \times \exp\left[-S_{cdom}\left(\lambda - 440\right)\right]$	(6)	[66]
Nap absorption	$a_{nap}\left(\lambda\right) = a_{nap}\left(440\right) \times \exp\left[-S_{nap} \times \left(\lambda - 440\right)\right]$ $a_{nap}\left(440\right) = a^*_{nap}\left(440\right) \times \left[SPM\right]$	(7)	[67]
Chla backscattering	$b_{b,chl}\left(\lambda\right) = \left\{0.002 + 0.01 \times \left[0.5 - 0.25 \times \log_{10}[C_{chl}] \times \left(\frac{\lambda}{550}\right)^n\right]\right\} \times b_{b,chl}\left(550\right)$ $b_{b,chl}\left(550\right) = 0.416 \times \left[Chl\right]^{0.766}$	(8)	[70]
NAP backscattering	$b_{nap}\left(\lambda\right) = b_{nap}\left(550\right) \times \left(\frac{550}{\lambda}\right)^{-\gamma} - \left[1 - \tanh\left(0.5 \times \gamma^2\right)\right] \times a_{nap}\left(\lambda\right)$ $b_{nap}\left(550\right) = b^*_{nap}\left(550\right) \times I \times \left[SPM\right]$	(9)	[69]
Scattering of water molecules	$b_{bw}\left(\lambda\right)$; Listed values, Table (3.8), page 104.	(10)	[71]
Absorption of water molecules	$a_w(\lambda)$; Listed values	(11)	[72]

In Table 2, $[Chl]$, $[SPM]$ and a_{cdom} (440) stand for Chla concentration, SPM concentration and the CDOM absorption at 440 nm respectively. The absorption and backscattering coefficients of water molecules (a_w and b_{bw}) were taken from previous studies (Mobley [71]; Pope and Fry [72]) and a_0 and a_1 were given in Lee et al. [67]. The initial values of non-algae particle absorption (a^*_{nap} (440) = 0.036 $m^2 \cdot g^{-1}$), spectral slope of non-algae particles (S_{nap} = 0.011 nm^{-1}), spectral slope of

CDOM (S_{cdom} = 0.013 nm^{-1}) and specific scattering coefficient of non-algae particles (b^*_{nap} (550) = 0.282) were taken from the Hommersom et al. [11] SIOP measurements at 37 stations in the Wadden Sea. Also, the initial values of γ and I (γ = 0.6 and I = 0.019) for the North Sea were taken from Doxaran et al. [69] and Petzold [73], respectively. In this study, we used the 2Seacolor forward model and the various parameterizations described in Table 2 to simulate the water-leaving reflectance (R_{RS} spectra) values for a series of combinations of Chla, SPM and CDOM concentration (Table 1) and for the given SZA associated with every MERIS image separately. The simulated values of R_{RS} spectra for all MERIS bands were stored in a water LUT for the MERIS bands and then used as R_{RS} input parameters for MODTRAN to calculate the TOA radiances in the MERIS bands.

3.1.2. Top of Atmosphere (TOA) Radiance Simulation by MODTRAN

MODTRAN is the successor of the atmospheric radiative transfer model LOWTRAN [74]. It is publicly available from the Air Force Research Laboratory in the USA. The latest version of MODTRAN (5.2.1) contains large spectral databases of the extraterrestrial solar irradiance and the absorption of all relevant atmospheric gases at a high spectral resolution. The accurate calculation of atmospheric multiple scattering makes it a very appropriate tool for reliable simulation and interpretation of remote sensing problems in the optical and thermal spectral regions [75]. To apply MODTRAN simulations, first of all several parameters describing the real atmospheric conditions should be determined as inputs for this model. Table 3 shows the standard definition of MODTRAN inputs with respect to the ranges of average values of atmospheric and geometric variables variation over one image for four years of all available MERIS images between 2007 and 2010 over the Dutch part of the Wadden Sea. In the MERIS image, some of the local atmospheric (O_3, H_2O) and geometric variables (VZA, SZA and RAA) can be used as input for MODTRAN. Note that for every MERIS image a separate input file was created by establishing the local atmospheric (O_3, H_2O, CO_2) and geometric variables (VZA, SZA, RAA) of that specific run to MODTRAN (Figure 3). These parameters could be retrieved from MERIS ancillary data per pixel using Matlab.

Table 3. Input parameters for MODTRAN4 simulations.

Parameter	Range or Value	Unit
Atmospheric profile	Mid Latitude Summer	-
Correlated-k option	Yes	-
DISORT number of streams	8	-
Concentration of CO_2 *	380–390	ppm
H_2O	0.5–4.5	$g{\cdot}cm^{-2}$
O_3	250–450	DU
SZA	30–80	degree
VZA	5–30	degree
RAA	0–150	degree
Visibility	5–50 (1 km increment)	km
Aerosol Model	Rural, Maritime, Urban	-
Surface height	0	km
Sensor Height	800	km
Molecular band model resolution	1.0	cm^{-1}
Start, ending wavelength	−1000	nm

* Annual CO_2 concentration level can be in Global Greenhouse Reference Network [76].

In this study, we varied the aerosol type (rural, maritime and urban) and visibility (5 to 50 km with 1 km step) and thus made a total of 135 scenarios for each lookup table and given atmospheric state and angular geometry, which were extracted from the MERIS image ancillary data per image. For each scenario the MODTRAN Interrogation Technique (MIT) was applied by using surface albedos of 0.0, 0.5 and 1.0 (the MIT is explained in detail by Verhoef and Bach [75]). The output .tp7 file of MODTRAN quantified the TOA radiance spectrum for each simulated wavelength from 350 to

1000 nm. Then in the MIT the .tp7 file was used as input to derive three MODTRAN parameters (gain factor (G), path radiance (L_0), and spherical albedo (S)). These parameters are spectral variables depending on various atmospheric conditions [75]. The spectral response functions (SRF) of the MERIS bands were convolved with the MODTRAN parameters to compute L_0, G and S for every MERIS band and these simulations were stored in the atmospheric LUTs (Atmos LUTs MERIS).

3.1.3. The MOD2SEA Retrievals

The simulated TOA radiance of MERIS data in the MODTRAN output file, L_{TOA} ($Wm^{-2}{\cdot}sr^{-1}{\cdot}\mu m^{-1}$), Can be expressed in surface reflectance r by the following equation [77]:

$$L_{TOA} = L_0 + \frac{Gr}{1 - Sr} \tag{12}$$

where r is the hemispherical reflectance ($=\pi R_{RS}$) leaving the water surface, L_0 is the total radiance for zero surface albedo ($Wm^{-2}{\cdot}sr^{-1}{\cdot}\mu m^{-1}$), S is the spherical albedo of the atmosphere and G is the overall gain factor. In this study, the LUTs of water-leaving reflectance generated by the 2SeaColor model were used as R_{RS} input parameters of Equation (12) to calculate TOA radiance for all combinations of water properties and atmospheric conditions and then organized in a water-atmosphere lookup table (water-atmosphere). The simultaneous retrieval of Chla, SPM, CDOM concentration, aerosol type and visibility was then performed by spectrally fitting the MOD2SEA-simulated TOA radiances (using RMSE) to MERIS TOA radiances for all MERIS bands except the band numbers 1, 2 and 11. Band 11 is located in the O_2-A absorption band and can give erroneous results due to sampling errors of MERIS. Bands 1 and 2 gave systematic deviations in R_{RS} after atmospheric correction. The cause of this problem is presently still unknown. In this retrieval, Chla retrieval using the coupled MOD2SEA model was performed in two steps. First the increments of 5, 5 and 1 were taken for Chla concentration ($mg{\cdot}m^{-3}$), SPM concentration ($g{\cdot}m^{-3}$) and CDOM absorption at 440 nm (m^{-1}), respectively, to find an approximate solution. Later, in the refined step, the step size of the LUTs composition was reduced to 0.1 for all water constituents in the identified rough range resulting from the first step. Applying this approach led to speeding up the running of the Matlab code and to obtaining more precise results. Although Figure 3 suggests the storage of a fixed LUT for water R_{RS} for each MERIS image, this LUT was only generated in a loop, and not stored, in order to reduce memory requirements. The best fitting combination of water properties and atmospheric conditions was found during the generation of the water LUT, but this water LUT was never stored as such, contrary to the atmospheric LUT, which was actually stored. This approach also allowed greater flexibility by applying the two-step procedure in finding the best-fitting water properties, by first applying a rough search in the first round with large steps in the three concentrations, and in the next round a refined search with small steps over much smaller ranges. It should be noted that the current procedure applied to a single pixel per matchup date is not suitable to be applied pixel by pixel, and this issue is left for a future study.

3.2. MERIS Case-2 Regional (C2R) Processor

The Case-2 regional processor (C2R) [42], available in the Basis ERS and ENVISAT (A) ATSR and MERIS Toolbox (BEAM) software, has been widely used to derive water quality parameters from MERIS images [78–81]. The C2R processor consists of two procedures, one for atmospheric correction and one for the bio-optical part for retrieving the IOPs of water columns. The Neural Networks (NN) in C2R were trained with Hydrolight [71] simulations and in situ measurements in the German bight and from other cruises in European seas [42]. More details can be found in Doerffer and Schiller [42]. The output of the C2R processor, including IOPs: the absorption coefficient of Chla at wavelength 443 nm (a_{chl} (443)), the absorption coefficient of CDOM (a_{CDOM} (443)), the total absorption (a_{tot} (443)), and the scattering coefficient of SPM (b_{spm} (443)) were then used to define water quality parameters

such as Chla and SPM. Equations to relate BEAM processor IOPs to water quality concentrations of Chla and SPM are presented as follows:

$$[\text{Chla}] = 21.0 \times a_{chl}(443)^{1.04} \quad (13)$$

$$[\text{SPM}] = 1.72 \times b_{spm}(443) \quad (14)$$

where [Chl], [SPM], a_{chl} (443) and b_{smp} (443) stand for Chla concentration, SPM concentration, the Chl absorption at 443 nm and SPM scattering coefficient at 443 nm, respectively.

3.3. Validation

To evaluate the accuracy of the MOD2SEA coupled model and the C2R processor, we applied these two models to the 35 matchup moments of MERIS observations and four years of concurrent Chla measurements (2007–2010) at the NIOZ jetty location, separately. The validation of model simulations were performed in two different levels of atmospheric correction and water retrieval models. Since the NIOZ jetty station is located close to the land, for every image, the darkest pixel from 5 by 5 pixels around the location of this station was extracted first. By selecting the darkest pixel from the 5×5 neighborhood centered on the jetty station, we exclude cloudy and land pixels, as well as water pixels close to the shore that are possibly influenced by an adjacency effect due to the near land area. Of course an underlying assumption in our approach is that the water of the darkest pixel has the same composition as found at the location of the jetty station. However, since the water current is mostly strong near the inlet to the Wadden Sea, we are confident that the water is well-mixed, and local gradients in water properties are small.

3.3.1. Atmospheric Correction

The accuracy of atmospheric correction methods using the coupled MOD2SEA model and C2R processor was evaluated against the ground truth water-leaving reflectance for all 35 matchups between 2007 and 2010 at the NIOZ jetty station. Four statistical parameters, the root mean square error (RMSE), the determination coefficient (R^2), the normalized root mean square error (NRMSE) and relative root mean square error (RRMSE) [82] were used to quantify the goodness-of-fit between derived and measured water-leaving reflectance values at the NIOZ jetty data where near-concurrent ($\pm$1 h) MERIS measurements were available. To do this, three MERIS bands 3, 5 and 7 were selected. Finally, the accuracy of the proposed MOD2SEA model in doing atmospheric correction was compared against C2R processor products. The results of this assessment are presented in Section 4.2.

3.3.2. Water Model Inversion

The accuracy of retrieved Chla concentration values using the coupled MOD2SEA model and the C2R processor were evaluated against ground truth Chla measurements for all 35 matchup points at the NIOZ jetty station between 2007 and 2010. The results of this evaluation are presented in Section 4.3. It should be mentioned that in view of the main objective of this study (retrieval of Chla concentration) and the availability of ground truth measurements, investigation of changes in other water constituents (SPM and CDOM concentration) was considered to fall outside of the scope of this study, although these were retrieved along with Chla using MOD2SEA. In addition, the visibility and aerosol type were retrieved simultaneously with water quality parameter concentration which were used in the model to simulate water-leaving reflectance values based on the best matching TOA radiance by MOD2SEA coupled model.

4. Results

4.1. Variability of MODTRAN Parameters (L_0, G and S) at Different Atmospheric Conditions

The case of the three aerosol types—rural, maritime and urban—for a visibility of 20 km on 7 October 2007 was used as an example to display the result of applying MODTRAN to the MERIS

bands for three atmospheric conditions. We used MIT method [75] to derive L_0, G and S values using surface albedos of 0.0, 0.5 and 1.0 for the mentioned visibilities and aerosol types in these figures.

The atmospheric path radiance L_0 represents the case when the surface reflectance is zero and the radiance at the top of atmosphere comes from atmospheric scattering alone. As Figure 4 shows, L_0 values decrease with wavelength, which means at longer wavelengths the atmosphere scatters less. The S presents the spherical albedo values which are not large and show a similar trend to L_0. The gain factor G contains the product of the extraterrestrial solar irradiance and the total two-way transmittance through the atmosphere, and shows a maximum at about 500 nm. L_0, S and G vary with different combinations of aerosol types and visibilities, while for maritime and rural aerosol types, they have similar values. The urban aerosol model has a stronger absorption and always has lower values when compared to the other two aerosol models. Examples of the MODTRAN path radiance simulations (L_0) from 7 October 2007, for visibilities of 5, 10 and 40 km while water-leaving reflectance is zero as representative for a range of haze conditions and three different aerosol models are presented in Figure 5.

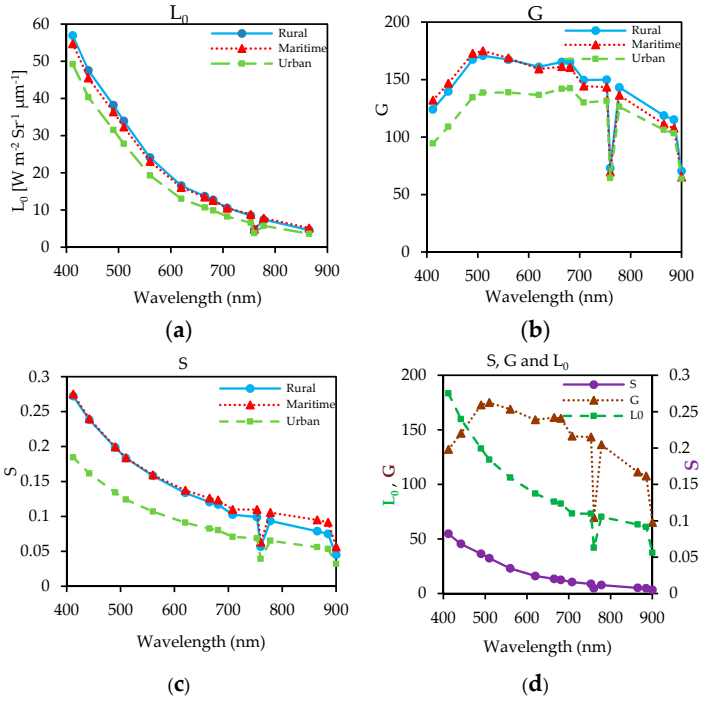

Figure 4. (**a**–**c**) L_0, G and S values at the visibility of 20 km and different aerosol types; (**d**) The atmospheric parameters L_0, S and G for the maritime aerosol type and a visibility of 20 km.

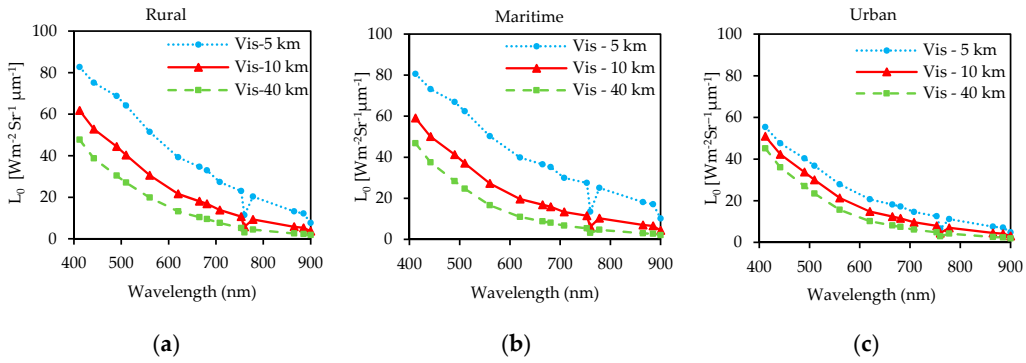

Figure 5. TOA radiance simulated by MODTRAN for (**a**) rural; (**b**) maritime and (**c**) urban aerosol types respectively.

As this figure shows, the calculated TOA radiances for the urban aerosol type show a lower range of variation compared to the maritime and rural cases. All the values of TOA radiance for the urban aerosol type are between 0 and 60 ($Wm^{-2}\cdot sr^{-1}\cdot \mu m^{-1}$), while these values for maritime and rural ones vary between 0 and 80 ($Wm^{-2}\cdot sr^{-1}\cdot \mu m^{-1}$). On the other hand, the simulated TOA radiances by MODTRAN differ significantly not only with aerosol type, but also with visibility. Lower visibility gives higher TOA radiances. Consequently, a wrong assumption about visibility or aerosol type leads to a wrong calculation of water-leaving reflectance and as a result the water parameter concentrations may be overestimated or underestimated.

4.2. Atmospheric Correction Validation

The results of performing of the coupled MOD2SEA model and the ESA MERIS standard C2R processor to derive water-leaving reflectances for MERIS bands of 3, 5 and 7 against ground truth measurements are shown in Figure 6. The statistical analysis regarding this assessment are presented in Table 4.

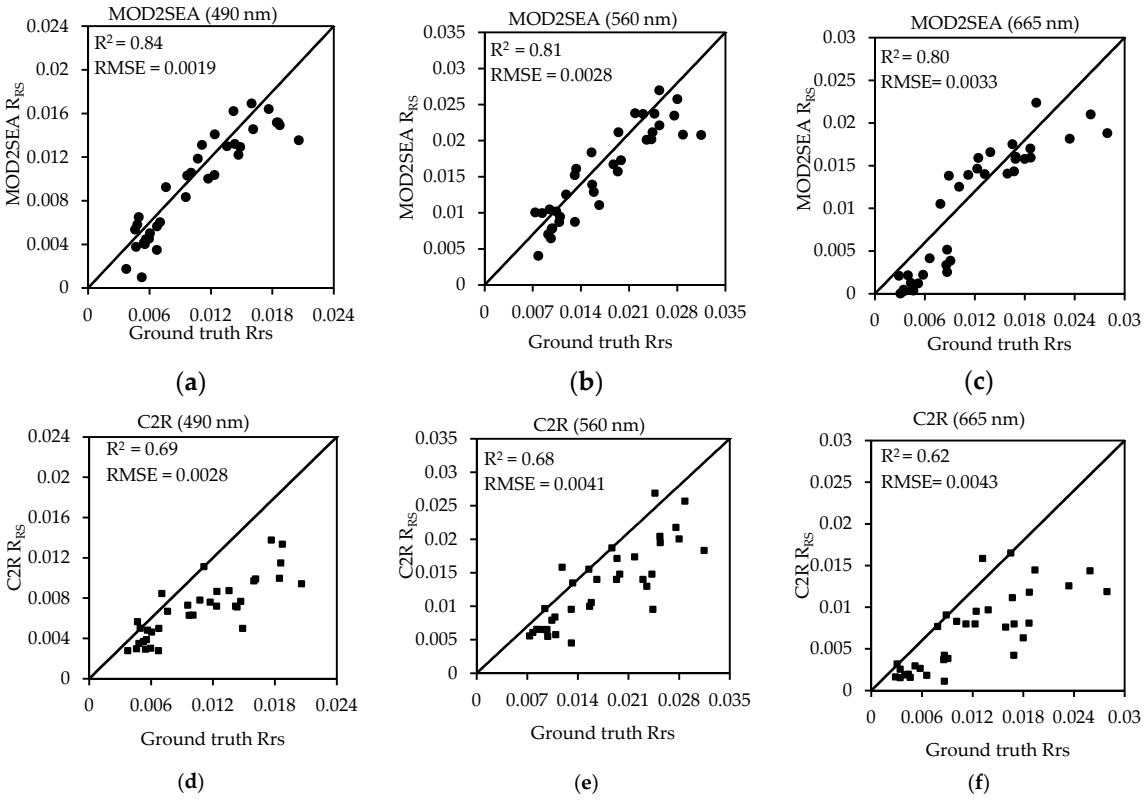

Figure 6. Comparison between MERIS-retrieved values and ground truth measurements for water-leaving reflectance values (Rrs) for 35 matchup in 2007−2010 at NIOZ jetty location. (**a**–**c**) represent the retrieved Rrs using the coupled MOD2SEA model against ground truth measurements for MERIS band of 3, 5 and 7 (band centers: 490, 560 and 665 nm) respectively; (**d**–**f**) represent the retrieved Rrs values using C2R processor against ground truth measurements for MERIS bands centers of 3, 5 and 7 (band centers: 490, 560 and 665 nm) respectively.

As it can be seen from Figure 6, the coupled MOD2SEA model provides significant improvements in the atmospheric correction and the resulting water-leaving reflectance in comparison with C2R processor in all MERIS bands of 3, 5 and 7. More details of this evaluation are presented in Table 4.

As the statistical measures show, performing atmospheric correction by applying the MODTRAN lookup table proposed in the MOD2SEA coupled model resulted in a reasonable accuracy against ground truth above the water radiometric dataset for 35 matchups between 2007−2010 at the NIOZ

jetty station for bands 3, 5 and 7 respectively. In addition, the MOD2SEA coupled model shows significant improvement especially in band 3 with R^2 = 0.84, RMSE = 0.0022, NRMSE = 13.18% and RRMSE = 21.08% in comparison with C2R. The standard C2R processor also shows higher accuracy for band 3 (R^2 = 0.69, RMSE = 0.0047) in comparison with bands 5 (R^2 = 0.68, RMSE = 0.0058) and 7 (R^2 = 0.62, RMSE = 0.0063), respectively.

Table 4. Models' performance evaluation in atmospheric correction part.

Statistical Measures	R^2		RMSE		NRMSE (%)		RRMSE (%)	
MERIS bands/Model	**MOD2SEA**	**C2R**	**MODSEA**	**C2R**	**MOD2SEA**	**C2R**	**MOD2SEA**	**C2R**
3	0.84	0.69	0.0022	0.0047	13.18	28.03	21.08	44.81
5	0.81	0.68	0.0034	0.0058	14.38	24.20	20.07	33.78
7	0.80	0.62	0.0035	0.0063	14.39	25.51	30.94	54.87

4.3. Water Retrieval Validation

The comparisons of C2R and MOD2SEA Chla retrieval against ground truth measurements are shown in Figure 7 and related statistical analysis are presented in Table 5.

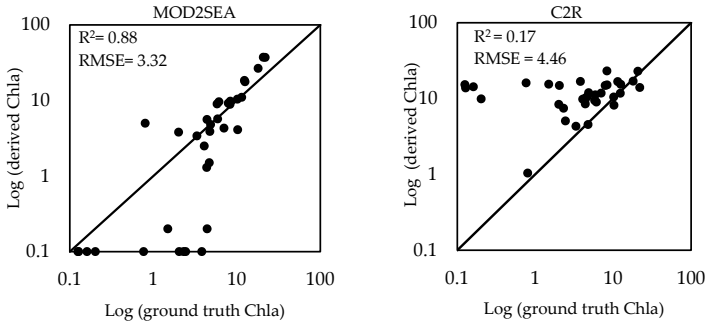

Figure 7. Comparison between MERIS-derived and measured log Chla (mg·m^{-3}) for 35 matchup moments. (**a**) MOD2SEA and (**b**) C2R.

Assessing the model accuracy using R^2 and RMSE shows the reasonable agreement between the measured and retrieved Chla (mg·m^{-3}) for all the matchup points during 2007–2010 at the NIOZ jetty location with a significant regression (Figure 7: R^2 = 0.88 and RMSE = 3.32 mg·m^{-3}) during the period of four years. In addition, the comparison of this model with the C2R processor shows significant improvement in retrieval of Chla. The result of this comparison is presented in Table 5.

Table 5. Models performance evaluation Chla retrieval.

Statistical Measures	R^2	RMSE	NRMSE (%)	RRMSE (%)
MOD2SEA	0.88	3.32	15.25	53.31
C2R	0.17	4.42	20.30	70.98

There are several possible reasons for the improvement of MOD2SEA in the retrieval of Chla in comparison with the C2R procedure, but the most obvious one is probably that the SIOPs used in the training of the C2R neural network might be more generic and thus different from the ones used in this study and which are more applicable to the Wadden Sea. In addition, the derived Chla data for 35 matchups between 2007–2010 by the MOD2SEA coupled model was examined to see how well the ground truth values (mg·m^{-3}) agreed with those derived from the MERIS images (mg·m^{-3}) at the NIOZ jetty location (Figure 8). In this figure, the X-axis presents the date while the Y-axis presents the

Chla concentration for ground truth data (in blue), the MOD2SEA coupled model (in red) between 2007 and 2010.

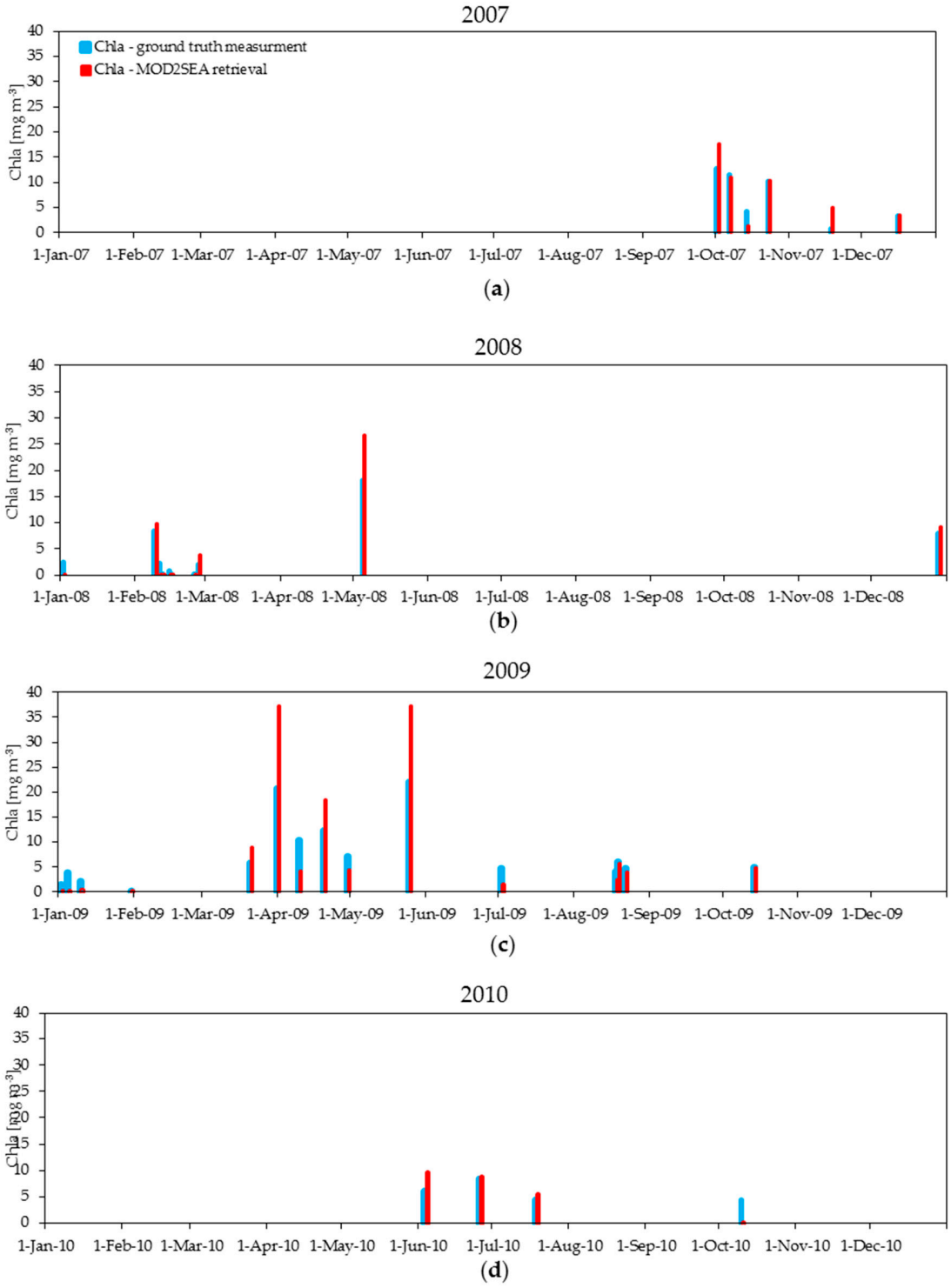

Figure 8. (**a**–**d**) The four-year comparison of derived Chla values using the coupled MOD2SEA model (red line) and ground truth measurements (blue line) ($mg \cdot m^{-3}$) from 2007−2010 at matchup moments.

As Figure 8 shows, the derived Chla concentration values using the MOD2SEA model shows reasonable agreement during 2007–2010, with maximum retrieved values of around 40 $mg \cdot m^{-3}$ and minimum values just above zero. However, despite the agreement between MERIS-derived and ground

truth Chla in a four-year period, systematic overestimations at high Chla concentration values (during April and May) mg·m^{-3} were also identified. Chla products, particularly during the phytoplankton bloom seasons of spring and summer, require further development. This overestimation might be explained by the Chla parametrization of the Lee et al. [68] model, since it appears that the Chla model calibration based on that model does not fit that well for the Wadden Sea. This Chla overestimation using satellite images was also in agreement with a Chla retrieval overestimation in most of the European seas studies by Zibordi et al. [58].

5. Discussion

Accurate estimation of water-leaving reflectance from satellite sensors is a fundamental goal for ocean color satellite missions [83]. Basically, the commonly applied atmospheric correction methods based on zero water-leaving reflectance in the near-infrared bands fail when applied to turbid waters since the high concentrations of water constituents lead to a detectable water-leaving reflectance in the near-infrared region in satellite image. In this study, we focused on the long-term retrieval of Chla concentration from MERIS images in the Wadden Sea, and the MOD2SEA coupled model is proposed as a tool to improve the retrieval of Chla concentration from earth observation data in this area.

Calculating accurate water-leaving reflectance spectra in order to translate them into Chla concentration under different atmospheric conditions is a crucial part of this study, since the atmosphere, in most cases, contributes more than 90% of the TOA radiance signal [41]. We can attribute the success of the MOD2SEA coupled model to its capability of combining simulations from 2SeaColor with the MODTRAN radiative transfer model for different combinations of aerosol type, visibility and water constituent concentrations for all MERIS bands to simulate TOA radiances, instead of applying routine atmospheric correction and water retrieval algorithms separately. Furthermore, based on a heterogeneous atmosphere assumption of the coupled MOD2SEA model, this technique can help suppress the influence of local haze variations in satellite images. Thus, applying this method results in a considerable improvement of the accuracy of the atmospheric correction, which is the most problematic part of remote sensing data processing for turbid waters like the Wadden Sea.

However, satellite estimation of Chla concentration is still difficult for coastal waters, where Chla, SPM and CDOM occur in various mixtures which complicate the derivation of their concentrations from reflectance observations. The 2SeaColor model performed well while the commonly applied water quality algorithms might fail in water constituent retrieval. Figure 9 shows an example of coupled MOD2SEA model spectral matchings for 2 October 2007.

As this figure shows, good matches are found between modelled and observed TOA radiance as well as modelled and atmospherically corrected water-leaving reflectance with respect to identified visibility and aerosol type by the coupled model. All in all, assessing the MOD2SEA Chla retrievals from MERIS data at one location (NIOZ jetty station) for a period of four years (2007–2010) shows reasonable agreement with ground truth measurements (R^2 = 0.88, RMSE = 33.2%). The 33.2% RMSE appears reasonable enough, as compared with the validation of the SeaWiFS Chla data product for global open ocean waters with a relative RMSE of about 58% [1]. In addition, this model shows considerable improvement to retrieve Chla concentration from satellite images in comparison with similar studies for the Wadden Sea [10,18]. The results of retrieved Chla concentration using this coupled model are within the range of measured Chla concentration (mg·m^{-3}) on the ground reported by other researchers, while a clear seasonal pattern is observed with the peak values during spring (in May). For example, Hommersom [10] reported Chla concentration range variations in the Wadden Sea during eight surface water sampling campaigns in 2006−2007 in 156 stations while Chla also showed a strong seasonal pattern with the highest values during spring in May. Chang et al. [84] showed the higher Chla concentrations occurred in May. Reuter et al. [85] provided continuous data on Chla concentration of the Wadden Sea at a time series station established in autumn 2002 by the University of Oldenburg. They reported a clear seasonal pattern in Chla concentration between 2007–2008 which has the highest values in May and the lowest values in November. Tillman et al. [86]

showed a large variability of Chla concentration over the year in the Wadden Sea. Winter concentrations were much lower than summer concentrations while in spring a phytoplankton bloom with peak concentrations occurs. Cadée and Hegeman [87] showed that yearly patterns of Chla concentration were similar in the Wadden Sea, although the overall inter-annual variability is large, as well as the maxima measured during spring bloom (in May). All in all, regarding the reasonable agreement of the MOD2SEA results with ground truth measurements and considering the turbid nature and complex heterogeneity in the turbid Wadden Sea, the performance of this coupled model should be regarded as encouraging and satisfactory enough.

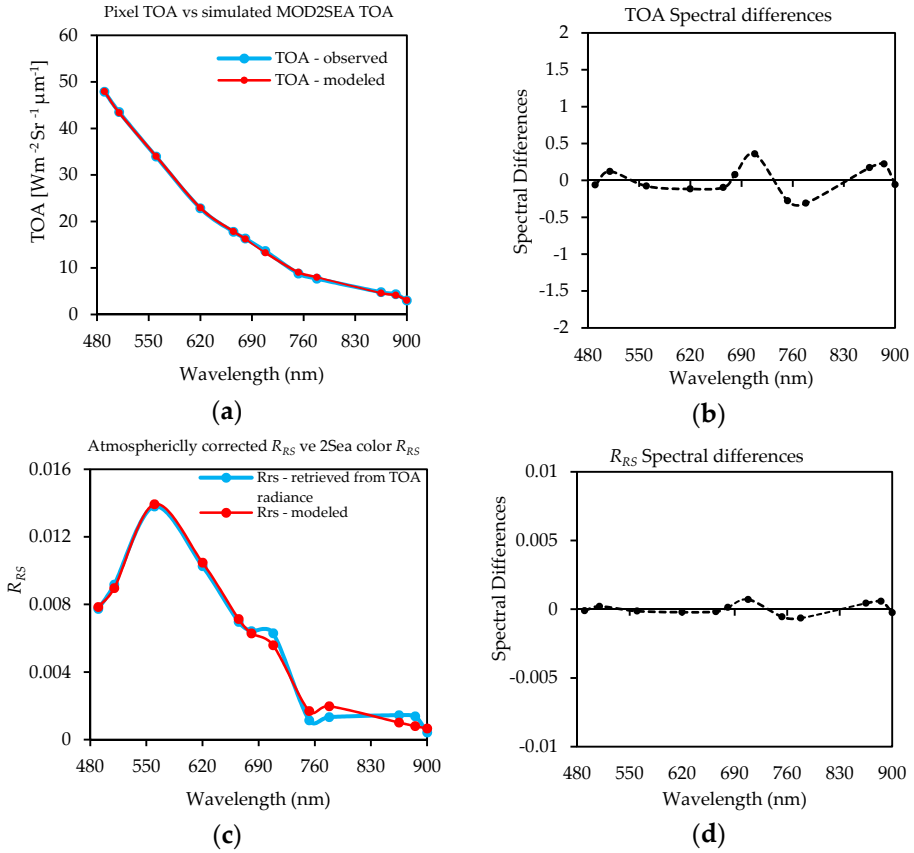

Figure 9. (**a**) The best match identified by the coupled model between simulated TOA radiances vs. pixel TOA radiance; (**b**) Spectral differences between observed and simulated TOA radiance; (**c**) The simulated R_{RS} (extracted from the best TOA radiance match) vs. the simulated 2SeaColor R_{RS}; (**d**) Spectral differences between simulated R_{RS} by 2SeaColor and atmospherically corrected R_{RS} from observed TOA radiance by MOD2SEA.

It is also worth mentioning that in shallow coastal waters like the Wadden Sea the bottom might influence the reflected signal to the sensor. This is not the case for the NIOZ jetty data where, due to the depth of >5 m and the high turbidity of the water (Table 1) near the NIOZ jetty and the surrounding area, the bottom effect on observed reflectance is negligible. This has been confirmed in the quality check of the NIOZ jetty data and the corresponding MERIS pixels. However, in the other shallower parts of the Wadden Sea, the bottom effect might contribute substantially in the visible region of the spectrum. As can be seen in Figure 1, the effect of the bottom is visible in large areas of the Wadden Sea satellite image. Thus, for shallow waters it is recommended in future studies to develop water constituent retrieval algorithms by incorporating sea bottom effects in the hydro-optical model. We speculate that developing a hydro-optical model including the bottom effect may lead to significant improvements in the derived water constituent concentrations from earth observation data in this

shallow coastal region. That is why, in the next phase of this research, we are going to include the bottom effect contribution into the TOA radiance calculation to derive and provide Chla concentration maps over the Wadden Sea.

For the Wadden Sea, and many other estuaries, knowledge of local specific inherent optical properties to locally calibrate retrieval algorithms is often lacking, and more research is still needed. For the Wadden Sea, Peters et al. [88] reported a complete set of SIOPs for Chla, SPM and CDOM measurements. However, the data of Peters were all collected at one location (the Marsdiep inlet) and only for two days (in May 2000). After that, the only published set of SIOP measurements in the Wadden Sea was constructed by Hommersom et al. [11]. Using Hommersom's measurements, SIOPs increased the accuracy of the derived Chla concentration significantly in comparison to previous efforts in this region. However, Hommersom's measurements lack seasonal information on the SIOPs while there is currently not much information on the SIOPs to be the basis for a hydro-optical model for the Wadden Sea. Without any doubt, having seasonal SIOPs may lead to an improved accuracy of retrieved Chla using this coupled model. Thus, more in situ data (especially on SIOPs) is still necessary for the model calibration.

Although our current efforts are centered on validating the proposed coupled atmospheric-hydroptical model in the highly turbid Wadden Sea using MERIS satellite images, it is unclear how broadly applicable this coupled model will be and to what extent these findings could be generalized. Thus, we suggest to extend this study to other parts of the world using various ocean color remote sensors. However, to apply this method to other regions, first the availability of valid SIOPs (water quality constituent's absorption and backscattering coefficient), in addition to the accurate ecological and geophysical knowledge of the interest area (i.e., the ranges of water constituent concentrations) are needed. Furthermore, spectral response functions of the desired sensor as well as atmospheric parameters and illumination geometry of the satellite image to run MODTRAN are required. As a consequence, access to accurate in situ water-leaving reflectance and water quality parameter concentration is essential for the assessment of primary data products from satellite ocean color missions [55] using the proposed approach.

The water Framework Directive regulations from the European Union force member states to monitor all their coastal areas (Environment Directorate-General of the European Commission, 2000). Availability of one decade of MERIS images (2002–2012) over the Wadden Sea, gives the opportunity to provide long-term Chla distribution maps using this coupled model with reasonable accuracy and to conduct a one-decade phenological analysis in this area. To provide Chla concentration maps with reasonable accuracy, the proposed method should be applied pixel by pixel for the whole region of interest. To speed up the pixel-based approach, a filter can be introduced to remove those combinations of visibilities and aerosol types from the MODTRAN lookup table which result in negative water-leaving reflectance values in any band, by considering the recorded TOA signal per pixel. On the other hand, other water quality parameters like SPM and CDOM as well as visibility and aerosol model maps can be produced as output of the MOD2SEA code. Of particular interest when analyzing the variability in the MERIS-derived Chla data trend for the Wadden Sea is whether any significant decreasing trend from 2002–2012 would indicate the effect of prior nutrient reduction management actions. This has significant implications for identifying positive anomaly events and may act as an alert for management actions. Clearly, climatic variability needs to be considered carefully when interpreting the long-term data trends and when making management decisions [1]. Furthermore, this established MERIS-based Chla data record may serve as baseline data to continuously monitor the estuary's eutrophic state, and the validated algorithm may extend such observations to the future using various satellite continuity missions. The Ocean Land Color Instrument (OLCI), embedded on the Sentinel-3 platform, is a sensor especially adapted for aquatic remote sensing [89] and succeeded the MERIS sensor in 2015 [90]. The launch of Sentinel-3 and OLCI will secure future consistent operational monitoring by medium resolution data for water quality assessment also of coastal zones and bays [89]. OLCI is designed mainly for global biological and

biochemical oceanography, which constrains its spatial resolution. On the other hand, the asymmetric view of OLCI will offer sun-glint free images in 21 spectral bands (from ultraviolet to near-infrared wavelengths) with an improved spatial coverage and temporal frequency. OLCI will provide high quality optical ocean observations (e.g., normalized water-leaving radiance, inherent optical properties, spectral attenuation of downwelling irradiance, photosynthetically active radiation, particle size distribution) and allow more accurate retrieval of the ocean color variables (e.g., Chlorophyll, SPM and CDOM concentrations) [91] where the OLCI bands are optimized to measure ocean color over open ocean and coastal zones. Sentinel-3 was successfully launched in February 2016 and will give free access to satellite data of the Wadden Sea. It is expected that the MOD2SEA coupled model will also operate successfully to derive Chla concentration using OLCI images for highly turbid waters and that it will result in an accuracy improvement in atmospheric correction and Chla retrieval aspects in comparison with the MERIS sensor. Thus, applying this method for further studies using OLCI data over the Wadden Sea is recommended.

6. Conclusions

A coupled atmospheric-hydro-optical model (MOD2SEA) has been proposed and validated to derive long-term Chla concentration ($mg \cdot m^{-3}$), visibility and aerosol type from MERIS observations for the coastal turbid area of the Wadden Sea. At one location, the model validation showed a good agreement between MERIS-derived and measured Chla concentration for a period of four years (2007–2010). We attribute the success of this approach to the simultaneous retrieval of atmosphere and water properties. In addition, we have found that water and atmospheric properties have different effects on TOA radiance spectra and therefore these are separately retrievable from MERIS data if the coupled MOD2SEA model is used. Using this coupled atmospheric-hydro-optical model led to considerable improvement for the simultaneous retrieval of water and atmosphere properties using earth observation data, with significant results in the accuracy in comparison with other algorithms applied to derive Chla in the Wadden Sea.

Acknowledgments: The authors would like to thank three anonymous reviewers for their constructive comments and suggestions to improve the quality of our paper. We also would like to thank the European Space Agency for providing the MERIS data within the framework of the "Integrated Network for Production and Loss Assessment in the Coastal Environment (IN PLACE)" project, which is funded by NWO-ZKO.

Author Contributions: All authors have made major and unique contributions in this research. The satellite data from ESA archive of MERIS images was provided by Suhyb Salama (as a part of IN PLACE project). Ground truth measurements from NIOZ jetty station were provided by Marcel Wernand. The Matlab code was written by Behnaz Arabi and Suhyb Salama and was then modified and extended by Wouter Verhoef. Behnaz Arabi performed in situ R_{RS} (λ), Chla and MERIS imagery categorization, matchup points finding, MODTRAN and model simulations, data analysis as well as the results interpretation. The original manuscript was written by Behnaz Arabi. In addition, Wouter Verhoef and Suhyb Salama supervised the research and discussed the results and provided substantial contribution in revising the manuscript at all stages. All co-authors participated in the improvement of the manuscript. All authors have read and approved the final version of this manuscript.

Conflicts of Interest: The authors declare no conflict of interest.

References

1. Le, C.; Hu, C.; English, D.; Cannizzaro, J.; Chen, Z.; Feng, L.; Boler, R.; Kovach, C. Towards a long-term chlorophyll-a data record in a turbid estuary using MODIS observations. *Prog. Oceanogr.* **2013**, *109*, 90–103. [CrossRef]
2. Casal, G.; Furey, T.; Dabrowski, T.; Nolan, G. Generating a Long-Term Series of Sst and Chlorophyll-a for the Coast of Ireland. *ISPRS Int. Arch. Photogramm. Remote Sens. Spat. Inf. Sci.* **2015**, *XL-7/W3*, 933–940. [CrossRef]
3. Werdell, P.J.; Bailey, S.W.; Franz, B.A.; Harding, L.W.; Feldman, G.C.; McClain, C.R. Regional and seasonal variability of chlorophyll-a in Chesapeake Bay as observed by SeaWiFS and MODIS-Aqua. *Remote Sens. Environ.* **2009**, *113*, 1319–1330. [CrossRef]
4. Moradi, M.; Kabiri, K. Spatio-temporal variability of SST and Chlorophyll-a from MODIS data in the Persian Gulf. *Mar. Pollut. Bull.* **2015**, *98*, 14–25. [CrossRef] [PubMed]

5. Peters, S.W.M.; Woerd, H.; Van der Pasterkamp, R. CHL maps of the Dutch coastal zone: A case study within the REVAMP project. *Structure* **2004**, *2003*, 10–13.
6. Van der Woerd, H.; Pasterkamp, R.; Van der Woerd, H.; Pasterkamp, R. Mapping the North Sea turbid coastal waters using SeaWIFS data. *Can. J. Remote Sens.* **2004**, *30*, 44–53. [CrossRef]
7. Le, C.; Hu, C.; English, D.; Cannizzaro, J.; Kovach, C. Climate-driven chlorophyll-a changes in a turbid estuary: Observations from satellites and implications for management. *Remote Sens. Environ.* **2013**, *130*, 11–24. [CrossRef]
8. Mélin, F.; Vantrepotte, V.; Clerici, M.; D'Alimonte, D.; Zibordi, G.; Berthon, J.-F.; Canuti, E. Multi-sensor satellite time series of optical properties and chlorophyll-a concentration in the Adriatic Sea. *Prog. Oceanogr.* **2011**, *91*, 229–244. [CrossRef]
9. Hommersom, A.; Wernand, M.R.; Peters, S.; De Boer, J. A review on substances and processes relevant for optical remote sensing of extremely turbid marine areas, with a focus on the Wadden Sea. *Helgol. Mar. Res.* **2010**, *64*, 75–92. [CrossRef]
10. Hommersom, A. "Dense water" and "Fluid Sand" Optical Properties and Methods for Remote Sensing of the Estremely Turbid Wadden Sea. Ph.D. Thesis, Vrije University Amsterdam, Amsterdam, The Netherlands, 2010.
11. Hommersom, A.; Peters, S.; Wernand, M.R.; de Boer, J. Spatial and temporal variability in bio-optical properties of the Wadden Sea. *Estuar. Coast. Shelf Sci.* **2009**, *83*, 360–370. [CrossRef]
12. Philippart, C.J.M.; Salama, M.S.; Kromkamp, J.C.; van der Woerd, H.J.; Zuur, A.F.; Cadée, G.C. Four decades of variability in turbidity in the western Wadden Sea as derived from corrected Secchi disk readings. *J. Sea Res.* **2013**, *82*, 67–79. [CrossRef]
13. Poremba, K.; Tillmann, U.; Hesse, K.-J. Distribution patterns of bacterioplankton and chlorophyll-a in the German Wadden Sea. *Helgol. Mar. Res.* **1999**, *53*, 28–35. [CrossRef]
14. Philippart, C.J.M.; Beukema, J.J.; Cadée, G.C.; Dekker, R.; Goedhart, P.W.; Van Iperen, J.M.; Leopold, M.F.; Herman, P.M.J. Impacts of nutrient reduction on coastal communities. *Ecosystems* **2007**, *10*, 95–118. [CrossRef]
15. Gemein, N.; Stanev, E.; Brink-spalink, G.; Wolff, J.-O.; Reuter, R. Patterns of suspended matter in the East Frisian Wadden Sea: Comparison of numerical simulations with MERIS observations. *Eur. Assoc. Remote Sens. Lab. Proc.* **2006**, *5*, 180–198.
16. Bartholdy, J.; Folving, S. Sediment classification and surface type mapping in the Danish Wadden Sea by remote sensing. *Neth. J. Sea Res.* **1986**, *20*, 337–345. [CrossRef]
17. Hommersom, A.; Researcher, I. A case study on the use of hydropt in the wadden sea. In Proceedings of the 2nd MERIS (A) ATSR User Workshop, Frascati, Italy, 22–26 September 2008.
18. Hommersom, A.; Peters, S.; Woerd, H.J.; Van der Eleveld, M.A. Tracking wadden sea water masses with an inverse bio-optical and endmember model satellite data. *EARSeL Proc.* **2010**, *9*, 1–12.
19. Schroeder, T.; Behnert, I.; Schaale, M.; Fischer, J.; Doerffer, R. Atmospheric correction algorithm for MERIS above case-2 waters. *Int. J. Remote Sens.* **2007**, *28*, 1469–1486. [CrossRef]
20. Gordon, H.R.; Wang, M. Retrieval of water-leaving radiance and aerosol optical thickness over the oceans with SeaWiFS: A preliminary algorithm. *Appl. Opt.* **1994**, *33*, 443–452. [CrossRef] [PubMed]
21. Goyens, C.; Jamet, C.; Schroeder, T. Evaluation of four atmospheric correction algorithms for MODIS-Aqua images over contrasted coastal waters. *Remote Sens. Environ.* **2013**, *131*, 63–75. [CrossRef]
22. Jamet, C.; Loisel, H.; Kuchinke, C.P.; Ruddick, K.; Zibordi, G.; Feng, H. Comparison of three SeaWiFS atmospheric correction algorithms for turbid waters using AERONET-OC measurements. *Remote Sens. Environ.* **2011**, *115*, 1955–1965. [CrossRef]
23. Siegel, D.A.; Wang, M.; Maritorena, S.; Robinson, W. Atmospheric correction of satellite ocean color imagery: the black pixel assumption. *Appl. Opt.* **2000**, *39*, 3582–3591. [CrossRef] [PubMed]
24. Carpintero, M.; Polo, M.J.; Salama, M.S. Simultaneous atmospheric correction and quantification of suspended particulate matter in the Guadalquivir estuary from Landsat images. *Proc. Int. Assoc. Hydrol. Sci.* **2015**, *368*, 15–20. [CrossRef]
25. Mélin, F.; Zibordi, G.; Berthon, J.-F. Assessment of satellite ocean color products at a coastal site. *Remote Sens. Environ.* **2007**, *110*, 192–215. [CrossRef]
26. Santer, R.; Schmechtig, C. Adjacency effects on water surfaces: Primary scattering approximation and sensitivity study. *Appl. Opt.* **2000**, *39*, 361–375. [CrossRef] [PubMed]
27. Sathyendranath, S. International ocean-colour coordinating group remote sensing of ocean colour in coastal, and other optically-complex. *Waters* **2000**, *3*, 2–11.

28. Hu, C.; Carder, K.L.; Muller-Karger, F.E. Atmospheric correction of SeaWiFS imagery over turbid coastal waters: A practical method. *Remote Sens. Environ.* **2000**, *74*, 195–206. [CrossRef]
29. Wang, M.; Shi, W. The NIR-SWIR combined atmospheric correction approach for MODIS ocean color data processing. *Opt. Express* **2007**, *15*, 15722–15733. [CrossRef] [PubMed]
30. Ruddick, K.G.; De Cauwer, V.; Park, Y.-J.; Moore, G.F. Seaborne measurements of near infrared water-leaving reflectance: The similarity spectrum for turbid waters. *Limnol. Oceanogr.* **2006**, *51*, 1167–1179. [CrossRef]
31. Wang, M. Remote sensing of the ocean contributions from ultraviolet to near-infrared using the shortwave infrared bands: Simulations. *Appl. Opt.* **2007**, *46*, 1535–1547. [CrossRef] [PubMed]
32. Wang, M.; Shi, W. Estimation of ocean contribution at the MODIS near-infrared wavelengths along the east coast of the U.S.: Two case studies. *Geophys. Res. Lett.* **2005**, *32*, 1–5. [CrossRef]
33. Wang, M.; Shi, W.; Tang, J. Water property monitoring and assessment for China's inland Lake Taihu from MODIS-Aqua measurements. *Remote Sens. Environ.* **2011**, *115*, 841–854. [CrossRef]
34. Salama, M.S.; Shen, F. Simultaneous atmospheric correction and quantification of suspended particulate matters from orbital and geostationary earth observation sensors. *Estuar. Coast. Shelf Sci.* **2010**, *86*, 499–511. [CrossRef]
35. Doxaran, D.; Lamquin, N.; Park, Y.-J.; Mazeran, C.; Ryu, J.-H.; Wang, M.; Poteau, A. Retrieval of the seawater reflectance for suspended solids monitoring in the East China Sea using MODIS, MERIS and GOCI satellite data. *Remote Sens. Environ.* **2014**, *146*, 36–48. [CrossRef]
36. Carder, K.L.; Cattrall, C.; Chen, F.R. MODIS clear water epsilons (ATBD 21). *Ocean. Color. Web.* **2002**, *2002*, 1–4.
37. Gould, R.W.; Arnone, R.A.; Martinolich, P.M. Spectral dependence of the scattering coefficient in case 1 and case 2 waters. *Appl. Opt.* **1999**, *38*, 2377–2383. [CrossRef] [PubMed]
38. Ruddick, K.G.; Ovidio, F.; Rijkeboer, M. Atmospheric correction of SeaWiFS imagery for turbid coastal and inland waters. *Appl. Opt.* **2000**, *39*, 897–912. [CrossRef] [PubMed]
39. Shen, F.; Verhoef, W.; Zhou, Y.X.; Salama, M.S.; Liu, X.L. Satellite estimates of wide-range suspended sediment concentrations in Changjiang (Yangtze) estuary using MERIS data. *Estuar. Coasts* **2010**, *33*, 1420–1429. [CrossRef]
40. Verhoef, W.; Bach, H. Coupled soil-leaf-canopy and atmosphere radiative transfer modeling to simulate hyperspectral multi-angular surface reflectance and TOA radiance data. *Remote Sens. Environ.* **2007**, *109*, 166–182. [CrossRef]
41. Shen, F.; Verhoef, W. Suppression of local haze variations in MERIS images over turbid coastal waters for retrieval of suspended sediment concentration. *Opt. Express* **2010**, *18*, 12653–12662. [CrossRef] [PubMed]
42. Doerffer, R.; Schiller, H. The MERIS Case 2 water algorithm. *Int. J. Remote Sens.* **2007**, *28*, 517–535. [CrossRef]
43. Duan, H.; Ma, R.; Simis, S.G.H.; Zhang, Y. Validation of MERIS case-2 water products in Lake Taihu, China. *GIScience Remote Sens.* **2012**, *49*, 873–894. [CrossRef]
44. Salama, M.S. *Roadmap Waterkwaliteit: Helder Beeld op Troebel Water*; ITC: Boston, MA, USA, 2014.
45. O'Reilly, J.E.; Maritorena, S.; Mitchell, B.G.; Siegel, D.A.; Carder, K.L.; Garver, S.A.; Kahru, M.; McClain, C. Ocean color chlorophyll algorithms for SeaWiFS. *J. Geophys. Res.* **1998**, *103*, 24937. [CrossRef]
46. O'Reilly, J.; Maritorena, S. Ocean color chlorophyll a algorithms for SeaWiFS, OC2, and OC4: Version 4. In *SeaWiFS Postlaunch Calibration and Validation Analyses*; NASA: Washington, DC, USA, 2000; pp. 8–22.
47. Dasgupta, S.; Singh, R.P.; Kafatos, M. Comparison of global chlorophyll concentrations using MODIS data. *Adv. Space Res.* **2009**, *43*, 1090–1100. [CrossRef]
48. Arnone, R.; Babin, M.; Barnard, A.H.; Boss, E.; Cannizzaro, J.P.; Carder, K.L.; Chen, F.R.; Devred, E.; Doerffer, R.; Du, K.; et al. *Remote Sensing of Inherent Optical Properties: Fundamentals, Tests of Algorithms, and Applications*; The International Ocean-Colour Coordinating Group: Dartmouth, NH, Canada, 2006.
49. Salama, M.S.; Radwan, M.; van der Velde, R. A hydro-optical model for deriving water quality variables from satellite images (HydroSat): A case study of the Nile River demonstrating the future Sentinel-2 capabilities. *Phys. Chem. Earth* **2012**, *50–52*, 224–232. [CrossRef]
50. Salama, M.S.; Verhoef, W. Two-stream remote sensing model for water quality mapping: 2SeaColor. *Remote Sens. Environ.* **2014**, *157*, 111–122. [CrossRef]
51. Ridderinkhof, H.; Zimmerman, J.T.F.; Philippart, M.E. Tidal exchange between the North Sea and Dutch Wadden Sea and mixing time scales of the tidal basins. *Neth. J. Sea Res.* **1990**, *25*, 331–350. [CrossRef]

52. Zibordi, G.; Berthon, J.F.; Mélin, F.; D'Alimonte, D. Cross-site consistent in situ measurements for satellite ocean color applications: The BiOMaP radiometric dataset. *Remote Sens. Environ.* **2011**, *115*, 2104–2115. [CrossRef]
53. Wernand, M.R.; Poseidon, S. Paintbox Historical Archives of Ocean Colour in Global-Change Poseidon's Verfdoos. Ph.D. Thesis, Utrecht University, Utrecht, The Netherlands, 2011.
54. Ly, J.; Philippart, C.J.M.; Kromkamp, J.C. Phosphorus limitation during a phytoplankton spring bloom in the western Dutch Wadden Sea. *J. Sea Res.* **2014**, *88*, 109–120. [CrossRef]
55. Zibordi, G.; Berthon, J.F.; Mélin, F.; D'Alimonte, D.; Kaitala, S. Validation of satellite ocean color primary products at optically complex coastal sites: Northern Adriatic Sea, Northern Baltic Proper and Gulf of Finland. *Remote Sens. Environ.* **2009**, *113*, 2574–2591. [CrossRef]
56. Schroeder, T.; Schaale, M.; Fischer, J. Retrieval of atmospheric and oceanic properties from MERIS measurements: A new Case-2 water processor for BEAM. *Int. J. Remote Sens.* **2007**, *28*, 5627–5632. [CrossRef]
57. Peters, S.W.M.; Eleveld, M.; Pasterkamp, R.; Van Der Woerd, H.; Devolder, M.; Jans, S.; Park, Y.; Ruddick, K.; Block, T.; Brockmann, C.; et al. *Atlas of Chlorophyll-a Concentration for the North; Sea Based on MERIS Imagery of 2003*; Vrije Universiteit: Amsterdam, The Netherlands, 2005.
58. Zibordi, G.; Mélin, F.; Berthon, J.F.; Canuti, E. Assessment of MERIS ocean color data products for European seas. *Ocean Sci.* **2013**, *9*, 521–533. [CrossRef]
59. Zibordi, G.; Mélin, F.; Berthon, J.F. Comparison of SeaWiFS, MODIS and MERIS radiometric products at a coastal site. *Geophys. Res. Lett.* **2006**, *33*, 1–4. [CrossRef]
60. Loisel, H.; Vantrepotte, V.; Jamet, C.; Dat, D.N. Challenges and new advances in ocean color remote sensing of coastal waters. In *Oceanography Research*; In Tech: Greer, SC, USA, 2013.
61. Duntley, S.Q. The optical properties of diffusing materials. *J. Opt. Soc. Am.* **1942**, *32*, 61–70. [CrossRef]
62. Duntley, S.Q. Light in the sea. *J. Opt. Soc. Am.* **1963**, *53*, 214–233. [CrossRef]
63. Morel, A.; Gentili, B. Diffuse reflectance of oceanic waters. II Bidirectional aspects. *Appl. Opt.* **1993**, *32*, 6864–6879. [CrossRef] [PubMed]
64. Lee, Z.; Carder, K.L.; Arnone, R.A. Deriving inherent optical properties from water color: A multiband quasi-analytical algorithm for optically deep waters. *Appl. Opt.* **2002**, *41*, 5755–5772. [CrossRef] [PubMed]
65. Salama, M.S.; Shen, F. Stochastic inversion of ocean color data using the cross-entropy method. *Opt. Express* **2010**, *18*, 479–499. [CrossRef] [PubMed]
66. Briucaud, A.; Morel, A.; Prieur, L. Absorption by dissolved organic matter of the sea (yellow substance) in the UV and visible domains. *Limnol. Oceanogr.* **1981**, *26*, 43–53. [CrossRef]
67. Lee, Z.; Carder, K.L.; Mobley, C.D.; Steward, R.G.; Patch, J.S. Hyperspectral remote sensing for shallow waters. I. A semianalytical model. *Appl. Opt.* **1998**, *37*, 6329–6338. [CrossRef] [PubMed]
68. Lee, Z.; Carder, K.L.; Mobley, C.D.; Steward, R.G.; Patch, J.S. Hyperspectral remote sensing for shallow waters. 2. Deriving bottom depths and water properties by optimization. *Appl. Opt.* **1999**, *38*, 3831–3843. [CrossRef] [PubMed]
69. Doxaran, D.; Ruddick, K.; McKee, D.; Gentili, B.; Tailliez, D.; Chami, M.; Babin, M. Spectral variations of light scattering by marine particles in coastal waters, from visible to near infrared. *Limnol. Oceanogr.* **2009**, *54*, 1257–1271. [CrossRef]
70. Morel, A.; Maritorena, S. Bio-optical properties of oceanic waters: A reappraisal. *J. Geophys. Res.* **2001**, *106*, 7163–7180. [CrossRef]
71. Mobley, C.D. *Light and Water: Radiative Transfer in Natural Waters*; Academic Press: Cambridge, MA, USA, 1994.
72. Pope, R.M.; Fry, E.S. Absorption spectrum (380–700 nm) of pure water. II. Integrating cavity measurements. *Appl. Opt.* **1997**, *36*, 8710–8723. [CrossRef] [PubMed]
73. Petzold, T. *Volume Scattering Functions for Selected Ocean Waters*; No. SIO-REF-72-78; Scripps Institution of Oceanography La Jolla Ca Visibility Laboratory: San Diego, CA, USA, 1972.
74. Kneizys, F.X.; Shettle, E.P.; Abreu, L.W.; Chetwynd, J.H.; Anderson, G.P. *Users Guide to LOWTRAN 7*; No. AFGL-TR-88-0177; Air Force Geophysics Lab Hanscom: Bedford, MA, USA, 1988.
75. Verhoef, W.; Bach, H. Simulation of hyperspectral and directional radiance images using coupled biophysical and atmospheric radiative transfer models. *Remote Sens. Environ.* **2003**, *87*, 23–41. [CrossRef]
76. Global Greenhouse Reference Network 2017. Available online: http://www.esrl.noaa.gov/gmd/ccgg/trends/ (accessed on 31 August 2016).

77. Berk, A.; Anderson, G.P.; Acharya, P.K.; Shettle, E.P. *MODTRAN 5.2. 1 User's Manual*; Spectral Sciences Inc.: Burlington, MA, USA, 2011.
78. Attila, J.; Koponen, S.; Kallio, K.; Lindfors, A.; Kaitala, S.; Ylöstalo, P. MERIS Case II water processor comparison on coastal sites of the northern Baltic Sea. *Remote Sens. Environ.* **2013**, *128*, 138–149. [CrossRef]
79. Beltrán-Abaunza, J.M.; Kratzer, S.; Brockmann, C. Evaluation of MERIS products from Baltic Sea coastal waters rich in CDOM. *Ocean Sci.* **2014**, *10*, 377–396. [CrossRef]
80. Smith, M.E.; Bernard, S.; O'Donoghue, S. The assessment of optimal {MERIS} ocean colour products in the shelf waters of the KwaZulu-Natal Bight, South Africa. *Remote Sens. Environ.* **2013**, *137*, 124–138. [CrossRef]
81. Ambarwulan, W.; Verhoef, W.; Mannaerts, C.M.; Salama, M.S. Estimating total suspended matter concentration in tropica coastal waters of the Berau estuary, Indonesia. *Int. J. Remote Sens.* **2012**, *33*, 4919–4936. [CrossRef]
82. Bayat, B.; Van der Tol, C.; Verhoef, W. Remote sensing of grass response to drought stress using spectroscopic techniques and canopy reflectance model inversion. *Remote Sens.* **2016**, *8*. [CrossRef]
83. Zibordi, G.; Ruddick, K.; Ansko, I.; Moore, G.; Kratzer, S.; Icely, J.; Reinart, A. In situ determination of the remote sensing reflectance: An inter-comparison. *Ocean Sci.* **2012**, *8*, 567–586. [CrossRef]
84. Chang, T.S.; Joerdel, O.; Flemming, B.W.; Bartholomä, A. The role of particle aggregation/disaggregation in muddy sediment dynamics and seasonal sediment turnover in a back-barrier tidal basin, East Frisian Wadden Sea, southern North Sea. *Mar. Geol.* **2006**, *235*, 49–61. [CrossRef]
85. Reuter, R.; Badewien, T.H.; BartholomÄ, A.; Braun, A.; Lübben, A.; Rullkötter, J. A hydrographic time series station in the Wadden Sea (southern North Sea). *Ocean Dyn.* **2009**, *59*, 195–211. [CrossRef]
86. Tillmann, U.; Hesse, K.-J.; Colijn, F. Planktonic primary production in the German Wadden Sea. *J. Plankton Res.* **2000**, *22*, 1253–1276. [CrossRef]
87. Cadée, G.C. Accumulation and sedimentation of Phaeocystis globosa in the Dutch Wadden Sea. *J. Sea Res.* **1996**, *36*, 321–327. [CrossRef]
88. Peters, S.W.M. *MERIMON-2000: MERIS for Water Quality Monitoring in the Belgian-Dutch-German Coastal Zone*; Food and Agriculture Organization of the United Nations: Rome, Italy, 2001.
89. Harvey, E.T.; Kratzer, S.; Philipson, P. Satellite-based water quality monitoring for improved spatial and temporal retrieval of chlorophyll-a in coastal waters. *Remote Sens. Environ.* **2014**, *158*, 417–430. [CrossRef]
90. Saulquin, B.; Fablet, R.; Bourg, L.; Mercier, G.; d'Andon, O.F. MEETC2: Ocean color atmospheric corrections in coastal complex waters using a Bayesian latent class model and potential for the incoming sentinel 3-OLCI mission. *Remote Sens. Environ.* **2016**, *172*, 39–49. [CrossRef]
91. Malenovský, Z.; Rott, H.; Cihlar, J.; Schaepman, M.E.; García-Santos, G.; Fernandes, R.; Berger, M. Sentinels for science: Potential of Sentinel-1, -2, and -3 missions for scientific observations of ocean, cryosphere, and land. *Remote Sens. Environ.* **2012**, *120*, 91–101.